

Far Infrared Absorption in Superconducting Lead Alloys*

J. D. LESLIE† AND D. M. GINSBERG

Department of Physics, University of Illinois, Urbana, Illinois

(Received 8 July 1963)

Measurements have been made at 1.3°K of the absorption of far infrared radiation in the surface of bulk samples of superconducting alloys composed of lead with various amounts of thallium, bismuth, or tin. The data provide the first direct experimental evidence for a sharp gap edge in superconducting alloys. The width of the energy gap decreases as thallium or tin is added to lead, and increases as bismuth is added. For concentrations up to 7.7 at. % thallium the fractional decrease in the gap width is approximately proportional to the fractional decrease in the critical temperature, but is significantly greater than the latter for 10.0 at. % thallium. The steepness of the absorption edge is roughly the same in all of the samples, and is greater than might have been expected from theoretical calculations, although these have only been performed in the extreme anomalous limit, which none of our samples strictly satisfy. The structure which was previously observed on the absorption curves of pure lead and mercury is also present in all of our alloys, indicating that it is probably not a result of anisotropy.

I. INTRODUCTION

A CONSIDERABLE amount of work has been devoted in recent years to the experimental determination of the width of the energy gap in various superconductors.¹ The motivation behind this work is provided by the fundamental nature of the gap, and its direct influence on many of the properties of superconductors.² The methods involve measurements of thermodynamic properties, energy absorption, electron tunneling, or transport phenomena. The results of these experiments have indicated that the reduced gap width $2\Delta/kT_c$ ranges from about 3.2 to 4.6, where 2Δ is the gap width, k is Boltzmann's constant, and T_c is the superconducting critical temperature. This range is in excellent but not perfect agreement with the theoretical value 3.5 which is predicted by the BCS theory.³ The explanation of the observed values of the gap width provides an intriguing fundamental problem. In an effort to help solve this problem, we have determined the energy gap in a series of alloys. It is hoped that the change in the size of the gap which occurs when the electronic properties of a metal are changed gradually by adding successively larger amounts of impurities will prove to be more easily understood than the variation of the gap width among pure metals, which differ from each other drastically in many of their properties. If this proves to be the case, an experimental study of alloys may provide an important step to our understanding of the deviation of the reduced gap width from the theoretical value. The measurements which we have made provide the first gap width determinations in

alloys, and indeed present the first direct experimental evidence for a well-defined gap width in superconducting alloys. This work also provides information concerning the subsidiary absorption peak below the main gap edge, which has been observed previously^{4,5} in pure lead and in mercury, as well as data which show the steepness of the absorption edge.

Section II is concerned with the experimental techniques. The results are presented and discussed in Sec. III, and the conclusions drawn from the data are summarized in Sec. IV.

II. EXPERIMENTAL PROCEDURE

A. General Remarks

One is required in performing this experiment to produce homogeneous samples of controlled composition, to expose them at low temperature (1.3°K in our experiments) to far infrared radiation of high purity, and to measure the absorption of this radiation in the surface of the samples. The methods which we have used were developed from those used in previous far infrared experiments on superconductors,^{4,5} with modifications which will be described.

B. Sample Preparation

A procedure was developed to produce the required homogeneous alloy samples. This is carried out as follows. The starting materials, which are indicated in

TABLE I. Sources and purity of metals.

Metal	Source	Stated purity
lead	American Smelting and Refining Co.	99.999+%
thallium	A. D. Mackay, Inc.	99.99%
tin	Vulcan Detinning Co.	99.99%
bismuth	American Smelting and Refining Co.	99.999+%

* Supported in part by the National Science Foundation, the Alfred P. Sloan Foundation, and the Air Force Office of Scientific Research.

† Present address: Physics Department, University of Waterloo, Waterloo, Ontario, Canada.

¹ D. H. Douglass, Jr. and L. M. Falicov, *Progress in Low Temperature Physics*, edited by C. J. Gorter (North-Holland Publishing Company, Amsterdam), Vol. IV (to be published).

² J. Bardeen and J. R. Schrieffer, in *Progress in Low Temperature Physics*, edited by C. J. Gorter (North-Holland Publishing Company, Amsterdam, 1961), Vol. III.

³ J. Bardeen, L. N. Cooper, and J. R. Schrieffer, *Phys. Rev.* **108**, 1175 (1957).

⁴ D. M. Ginsberg and M. Tinkham, *Phys. Rev.* **118**, 990 (1960).

⁵ P. L. Richards and M. Tinkham, *Phys. Rev.* **119**, 575 (1960).

Table I, are weighed out for a desired alloy in the required proportion, and are placed in a clean Pyrex tube. This is then evacuated to 10^{-5} Torr and sealed off. The tube is heated up to melt the metal which is inside, and the ingredients are thoroughly mixed by vigorously agitating the tube. The tube is then cooled as quickly as possible in a blast of compressed air. The resulting alloy ingot is removed from the tube, and is cut up and placed in the ingot chamber of a carefully cleaned demountable mold, which is shown in Fig. 1. (The mold is made of a high grade of pure iron, called Meehanite,⁶ which is very highly insoluble in the metals which are cast.⁷ A thin coating of colloidal carbon⁸ keeps the cast sample from sticking to the surface of the mold.) With the ingot chamber downward, the mold is placed into a furnace tube, made of monel, which is then placed into a tubular furnace. The furnace tube is evacuated to 10^{-5} Torr and then heated up to a temperature about 40°C above the melting point of the alloy. After the molten metal has outgassed and the pressure has returned to 10^{-5} Torr, the furnace is lowered away from the furnace tube, which is then agitated and inverted without breaking the vacuum. (This makes use of a rotating vacuum joint.) The metal runs down into the conical sample chamber and the wire sample chambers shown in Fig. 1. (We will describe later the use of the wire samples.) Gaseous helium is admitted into the furnace tube, which is then quickly dismantled so that the mold can be quenched to room temperature in distilled water. A thermocouple which is attached to the mold during the heating and cooling process produces a voltage which is continuously displayed on a chart recording. This is later examined to confirm that the mold had not cooled to the alloy's liquidus before the quenching was carried out. It is hoped that the rapid quenching, which is aided by the smallness of the mold's mass (615 g), prevents large-scale inhomogeneities from developing as the alloys cool through the temperature range of solidification. After removing the sample from the mold and etching the surface heavily in hydrochloric acid to remove surface contamination, a further attempt to promote homogeneity is made by annealing each sample in an evacuated, sealed-off Pyrex tube at a temperature about 30°C below the solidus of the alloy for three to four months. The etch patterns on the surfaces of the samples indicate crystals which range in size from a few mm to about 1 cm. The sharpness of the superconducting energy gap edges which our infrared measurements reveal indicates that the sample-making techniques have actually succeeded in producing highly homogeneous samples, at least on a scale of the superconducting coherence length.

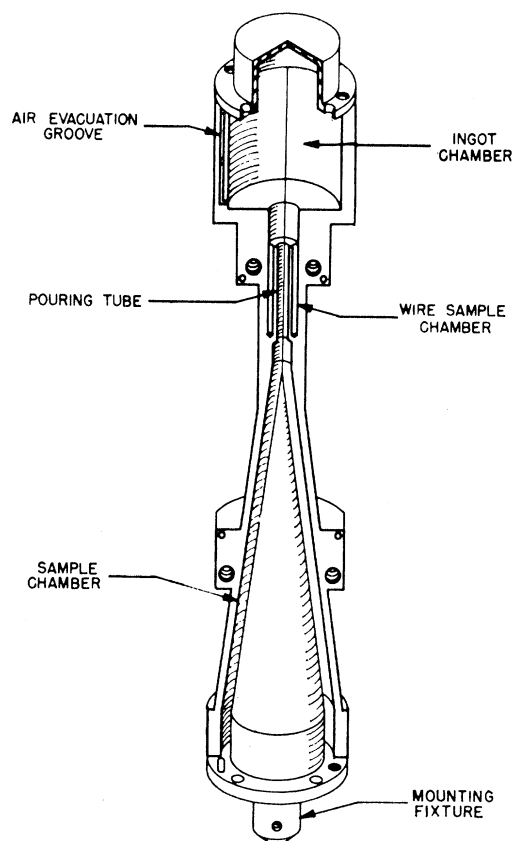


Fig. 1. Demountable mold used in casting the conical cavity sample and the wire samples.

The compositions of our samples are given in Table II. (The other entries in the Table will be discussed later. The derivation of some of the parameters is given in the Appendix.)

C. Radiation Production and Detection, and Low-Temperature Techniques

The techniques used to generate, isolate, and detect the far infrared radiation which is used in this experiment are essentially the same as those used in previous experiments, to which the reader is referred for some of the details.^{4,5} The source is a high-pressure mercury arc, and gratings and transmission filters are used to select the wavelength desired, and to remove undesired short-wavelength radiation. The beam is chopped at 39 cps before entering a brass light pipe which conducts it down into the low-temperature equipment. At the lower end of a Pyrex helium Dewar, it is funneled by a brass cone into an oversized nonresonant cavity, which is made of the alloy under investigation. This is shown in Fig. 2. A carbon bolometer in the cavity measures the energy density, and generates a 39 cps electrical signal which is amplified and detected by means of a conventional lock-in amplifier. The bolometer signal is partially

⁶ Purchased from Banner Iron Works, St. Louis, Missouri.

⁷ M. Hansen, *Constitution of Binary Alloys* (McGraw-Hill Book Company, Inc., New York, 1958).

⁸ Dag Dispersion No. 154, Acheson Colloids Company, Port Huron, Michigan.

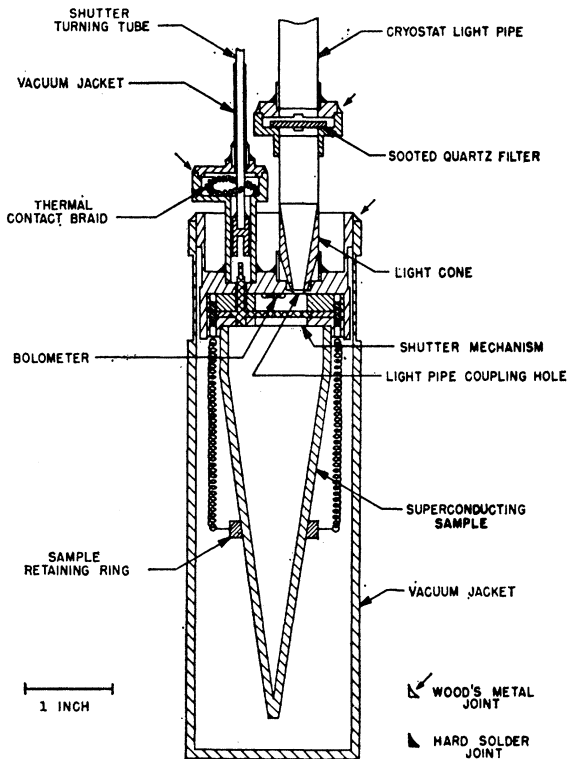


FIG. 2. Conical sample cavity and holder used in making far infrared measurements.

determined by the absorption of the radiant energy in the walls of the cavity, which is the phenomenon of interest. (The manner in which this absorption is isolated from extraneous factors which affect the bolometer signal will be described in the next section.) The carbon bolometer is somewhat novel in the design of its electrodes.⁹ These are made by using a flexible silver paint¹⁰ to glue No. 36 Advance¹¹ wires to the bolometer. The electrodes are protected by a coating of Epibond 104¹² applied over the silver paint, and seem to be somewhat quieter than evaporated indium electrodes, which were used previously.

During the experimental measurements, the space around the sample and bolometer is evacuated. The thermal contact between the sample and the helium bath outside of the vacuum jacket is provided by a heavy copper braid, which is soft-soldered to the vacuum jacket and attached to the sample by a Wood's metal joint. This braid is not shown in Fig. 2.

The shutter which is shown in Fig. 2 is operated from the top of the cryostat. With this shutter closed, the superconducting sample is completely hidden from the

radiation and bolometer, and we obtain a reference signal which indicates the over-all sensitivity of the equipment. When the shutter is opened, the radiation can enter the superconducting cavity unhindered, and has to make many bounces off the sample walls before reaching the bolometer.

D. Method of Making the Measurements

The bolometer signal is determined not only by the absorption in the cavity walls, but by extraneous factors, which are variations in the source intensity, the losses in the optical system, the sensitivity of the bolometer, and the gain of the electronic amplifying equipment. In order to obtain information about the factor of interest, which is the absorptivity of the cavity walls, we force the cavity into the normal state by applying a magnetic field, which in our experiments is 3000 Oe. The ratio of the bolometer signal when the cavity walls are superconducting to the signal when the walls are normal would provide information which is unaffected by the extraneous factors just mentioned if those factors did not vary during the time required to measure these two signals. However, since superconducting alloys trap a large amount of magnetic flux, we are forced to take all of our readings with the cavity superconducting in a given run before taking the normal-state readings for that run. The extraneous factors which influence the bolometer signal vary during the run, so the sensitivity of the equipment must be continuously monitored. This we do by alternately making measurements with the shutter open and measurements with the shutter closed. (The shutter is described in the previous section.) We standardize all of our readings by dividing the average of three determinations of the bolometer signal obtained with the shutter open by the average of three alternating determinations of the bolometer signal obtained with the shutter closed. The resulting ratio is called P_S or P_N , depending on whether the cavity was in the superconducting state or the normal state, respectively. Each chart recording is taken for a period of about six time constants of the lock-in amplifier. The time constant ranges from 10 sec for the quietest signals to 120 or even 240 sec for the noisiest signals. This entire process is repeated a number of times, ranging usually from 3 to 8 for each wavelength, some of the repetitions occurring on different runs.

For two of the samples, numbers 6 and 10, the maximum field available, 3000 Oe, was insufficient to completely quench the superconductivity according to the infrared measurements, so for these we obtained significant data only with the sample superconducting.

We attempted to measure the residual resistances of our samples at 4.2°K in a field of 3000 Oe by using some of the wire samples which were cast and annealed with our cavity samples. One would expect the residual resistances of the samples to increase linearly with

⁹ J. D. Leslie, Ph.D. thesis, University of Illinois, 1963 (unpublished).

¹⁰ SC-13 silver micropaint, Micro-Circuits Company, New Buffalo, Michigan.

¹¹ Driver-Harris Company, Harrison, New Jersey.

¹² Furane Plastics, Los Angeles, California.

TABLE II. Sample compositions and characteristics.

Sample No.	Solute	at.% Solute	2Δ cm^{-1}	ρ Ω cm	L \AA	ξ \AA	$\omega\tau$	λ/ξ	K
1	thallium	1.00	21.65 ± 0.3	0.61	1700	580	1.3	0.73	4.673
2	thallium	3.08	21.5 ± 0.3	1.91	560	380	0.42	1.3	2.950
3	thallium	5.3	21.6 ± 0.4	3.25	330	280	0.25	2.0	5.263
4	thallium	7.7	21.2 ± 0.3	4.71	230	220	0.17	2.8	3.774
5	thallium	10.0	19.6 ± 0.3	6.00	180	180	0.13	3.5	1.808
6	thallium	50.0	...	23.8	44	55	0.034	21.	0.948
7	bismuth	0.01	21.8 ± 0.5	0.0113	94 000	780	71.	0.51	6.803
8	bismuth	0.2	21.7 ± 0.3	0.226	4700	690	3.5	0.57	4.878
9	bismuth	6.0	22.0 ± 0.3	6.77	160	160	0.12	4.0	2.915
10	bismuth	16.0	22.3 ± 0.3	16.0	66	79	0.050	12.	2.398
11	tin	4.0 ^a	21.4 ± 0.3	1.1	970	480	0.73	0.94	8.130
12	tin	10.0 ^a	21.5 ± 0.3	6.329

^a Probably precipitated to 3.5 at. % tin in lead.

alloying. However, we found that most of our samples had low-temperature resistances which were lower than that of our almost pure lead sample (Number 7, 0.1 at.% Bi in Pb). Moreover there was no apparent systematic variation of the measured residual resistance as a function of alloying. Since a chemical analysis which was made on a portion of two of our samples has shown that the intended compositions were in fact achieved, this discrepancy cannot be blamed on unexpected sample compositions. It seems certain that some superconducting filaments were present in our alloy samples, even in the presence of the applied magnetic field, and that these filaments masked the change in normal-state

dc resistance which alloying produced. Such filaments have been noted in superconducting alloys by many investigators.

E. Data Analysis

The data for a sample are processed in the following way to yield an absorption curve. From the values of $P_S(\nu)$ obtained for a given wave number ν in different runs, we compute an average value $[P_S(\nu)]_A$. The values of this average for different ν are then normalized so that $P_S(33.33 \text{ cm}^{-1})=1$, to yield the normalized values $[P_S(\nu)]_{A,n}$. Then the same process is carried out for the normal-state data. Finally, each "superconducting" value $[P_S(\nu)]_{A,n}$ is divided by the corresponding "normal" value $[P_N(\nu)]_{A,n}$. The resulting ratios are plotted as a function of ν , and a curve is drawn through the points. The energy at which the curve seems to have a discontinuity in slope is taken to be the width of the energy gap, 2Δ .

To facilitate comparison of the shape of the various absorption curves, the following final normalization is made. We calculate

$$P(\nu) = K \left\{ \frac{[P_S(\nu)]_{A,n}}{[P_N(\nu)]_{A,n}} - 1 \right\},$$

where K is chosen so that the height of the absorption curve at the energy gap is unity. The values of K used in this process are listed in Table II. The absorption curves then show how $P(\nu)$ depends on ν .

The above procedure was carried out for all of the samples, except that for numbers 6 and 10, $[P_N(\nu)]_{A,n}$ was taken to be unity for all the values of ν , since we have no normal-state data for these samples, as explained above. The ordinates of the absorption curves for these two samples are labeled P^* to call attention to this. Also, since the absorption data for sample 6 did not allow the clear assignment of an energy gap value, the curve is arbitrarily normalized to have unit height at 12.0 cm^{-1} .

The uncertainty indicated by the vertical line drawn through each point determining the absorption curves

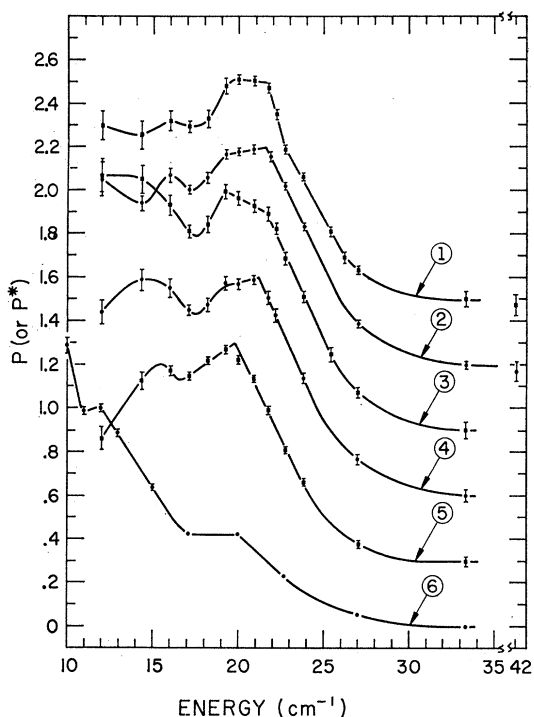


FIG. 3. Absorption curves for samples 1 through 6. Sample compositions are given in Table II. For samples 1 through 5, P is plotted. For sample 6, no normal-state data could be obtained, so P^* is plotted. P and P^* are defined in the text (Sec. II.E).

indicates plus and minus one standard deviation $S(\nu)$, as computed from a statistical analysis⁹ of the relative scatter in values of P from data obtained on six of the samples.

III. EXPERIMENTAL RESULTS AND DISCUSSION

A. The Data

The absorption curves are presented in Figs. 3 and 4. The meaning of P or P^* , and the manner in which the experimental uncertainties were estimated, is discussed above. It can be shown⁵ that P is approximately proportional to $R_N - R_S$, where R_N and R_S are the surface resistances of the sample in the normal and superconducting state, respectively. The numerical data from which the curves have been plotted are tabulated elsewhere.⁹

All the absorption curves except that for sample 6 show sharp absorption edges. (The interpretation of the absorption curve for sample 6 is difficult, since we have no normal-state absorption data.) The absorption curves all show at least one small absorption peak below the main absorption edge. This structure will be discussed in Sec. III.E.

The energy gap 2Δ is taken to be the energy at which the absorption curve seems to have a discontinuity in slope. Uncertainties were assigned to the gap values by

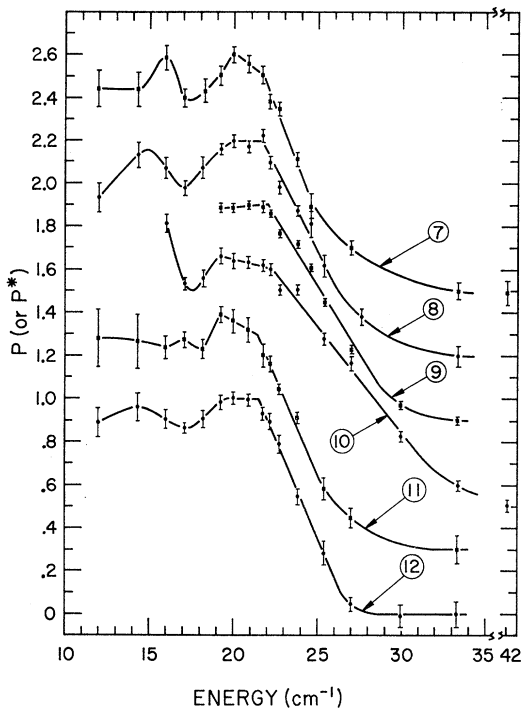


FIG. 4. Absorption curves for samples 7 through 12. Sample compositions are given in Table II. All of the plotted points indicate values of P , except for sample 10. For the latter, no normal-state data could be obtained, so P^* is plotted. P and P^* are defined in the text (Sec. II.E).

passing possible curves through the error bars. The gap width values and their uncertainties are listed in Table II.

B. Comparison of Gap Widths with Other Experiments

For the lead-thallium system, our energy gap values can be compared with reliable critical temperature measurements. Finnemore and Mapother¹³ have made magnetic measurements on some of the wire samples which were cast and annealed with our cavity samples. Their measurements yield the difference between T_c of an alloy sample and that of a pure lead reference sample. Using the critical temperature value for pure lead obtained by Franck and Martin,¹⁴ they then obtain the critical temperatures indicated by Fig. 5. In this Figure, we have compared the effect which the thallium impurity has on 2Δ with its effect on T_c by plotting

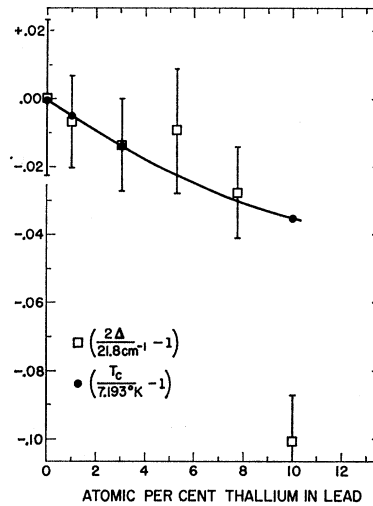


FIG. 5. Effect of thallium impurity on the energy gap width 2Δ and the critical temperature T_c of lead.

$[(2\Delta/21.8 \text{ cm}^{-1}) - 1]$ and $[(T_c/7.193^\circ\text{K}) - 1]$ versus at. % thallium, where 21.8 cm^{-1} and 7.193°K are the pure-lead values of 2Δ and T_c . As evidenced by the plot, the reduced gap width $2\Delta/kT_c$ remains approximately constant up to 7.7 at. % thallium, within the uncertainties of the experimental results. (The uncertainty in T_c is negligible compared with that in 2Δ .) However for 10 at. % thallium, the fractional decrease in energy gap is significantly larger than the fractional decrease in critical temperature. There is some evidence,¹⁵ although not conclusive, that we may have crossed a band edge in going from 7.7 to 10 at. % thallium. If this is the case, it might account for the sudden change in $2\Delta/kT_c$.

In Fig. 6 we have plotted $[(2\Delta/21.8 \text{ cm}^{-1}) - 1]$ versus impurity content for our lead-bismuth and lead-tin

¹³ D. K. Finnemore and D. E. Mapother (to be published).

¹⁴ J. P. Franck and D. L. Martin, Can. J. Phys. **39**, 1320 (1961).

¹⁵ A. V. Gold, Phil. Mag. **5**, 70 (1960).

samples. Unfortunately, we know of no reliable critical temperature measurements for either of these alloy systems to compare with our gap values. Meissner *et al.*¹⁶ obtained critical temperature data for lead-bismuth and lead-thallium alloys by measuring the resistive transition, but this is now known to be an unreliable method. In Fig. 6, the energy gap appears to be increasing linearly with the amount of bismuth impurity. Meissner *et al.* found an increase in the critical temperature as lead is alloyed with bismuth, but their fractional changes in T_c are about five times larger than our fractional changes in energy gap.

The concentrations of our two lead-tin samples are shown in Fig. 6 as 4.0 and 10.0 at.%, but there is strong evidence from magnetic data of Livingston¹⁷ that all but about 3.5 at.% of the tin in these samples precipitated out of the solid solution before the infrared measurements were made. Therefore, these two samples most likely have a composition of 3.5 at.% tin in lead, with different amounts of precipitated tin. It is interesting that the absorption curves for both of these samples have sharp gap edges.

The trends shown by the data of Figs. 5 and 6 are similar to those noted by Serin and coworkers^{18,19} in an extensive and systematic set of measurements of the critical temperatures of tin and aluminum alloys. They observed that large concentrations of solute impurities with higher valence than the host metal tend to raise T_c more than those of the same valence, which in turn tend to raise T_c more than impurities of lower valence.

C. Comparison of Gap Widths with Theory

We know of three detailed calculations of the effect of the electron mean free path on the superconducting energy gap. One of these²⁰ is limited to much smaller impurity concentrations than are present in our samples. The other two^{21,22} predict a decrease in the gap width which is an order of magnitude larger than that observed in the thallium-doped alloys. However, these two calculations seem to be made invalid by the following theoretical considerations. Mattis and Bardeen²³ and also Anderson²⁴ have pointed out that the pairing in the presence of impurities should be between exact time-reversed eigenstates of the normal-state alloy. Anderson has also emphasized the importance of carefully handling the energy cutoff of the electron-phonon interaction. He has shown that the limitation

¹⁶ W. Meissner, H. Franz, and H. Westerhoff, *Ann. Physik* **13**, 505 (1932).

¹⁷ J. D. Livingston (private communication).

¹⁸ E. A. Lynton, B. Serin, and M. Zucker, *J. Phys. Chem. Solids* **3**, 165 (1957).

¹⁹ E. A. Lynton and B. Serin, *Phys. Rev.* **112**, 70 (1958).

²⁰ D. J. Kenworthy and D. ter Haar, *Phys. Rev.* **123**, 1181 (1961); see erratum: D. J. Kenworthy, M. J. Zuckermann, D. M. Brink, and D. ter Haar, *Phys. Letters* **1**, 35 (1962).

²¹ H. Suhl and B. T. Matthias, *Phys. Rev.* **114**, 977 (1959).

²² K. Nakamura, *Progr. Theoret. Phys. (Kyoto)* **21**, 435 (1959).

²³ D. C. Mattis and J. Bardeen, *Phys. Rev.* **111**, 412 (1958).

²⁴ P. W. Anderson, *J. Phys. Chem. Solids* **11**, 26 (1959).

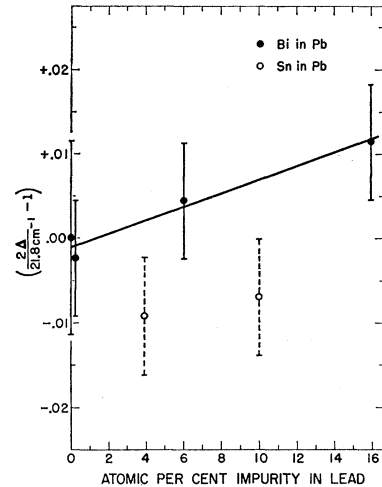


FIG. 6. Effect of bismuth or tin impurity on the energy gap width 2Δ of lead.

of the electron mean free path L by the addition of impurities should not change the gap width or critical temperature if one starts the calculation with an electron-phonon interaction which is isotropic in the pure superconductor. The experimentally observed initial decrease in T_c which is brought about by small amounts of impurities^{18,19} is attributed by Anderson to a washing out of the anisotropy which is actually present in the pure superconductor.

The solutes are also expected to bring about changes in other parameters which affect the critical temperature and energy gap. These are evident in the relation which BCS derive³ for the pure isotropic superconductor (in the weak-coupling limit)

$$2\Delta = 3.5kT_c = 4.0\hbar\omega_p \exp(-1/NV). \quad (1)$$

In this equation, $\hbar\omega_p$ is some average phonon energy, N is the density of states at the Fermi surface in the normal metal, and V is the electron-phonon coupling constant. Unfortunately, there are neither experimental data nor convincing theoretical results which tell us how the phonon spectrum is changing as one adds impurities to lead. Also, there are conflicting claims,²⁵⁻²⁷ based on experimental measurements on other alloy systems, concerning the question of how, or even whether, the coupling constant V changes with alloying. There is some evidence¹⁵ that the density of states N may be increasing as one adds bismuth to lead, and decreasing as one adds thallium to lead, and this would, according to Eq. (1), lead to a change in gap width of the observed sign. In the present circumstances, it would be premature to make a quantitative comparison, however, particularly in light of indications from magnetic measurements²⁸ that N does not change with the addition of bismuth or thallium to lead.

²⁵ R. I. Gayley, Jr., E. A. Lynton, and B. Serin, *Phys. Rev.* **126**, 43 (1962).

²⁶ C. H. Cheng, K. P. Gupta, E. C. Van Reuth, and Paul A. Beck, *Phys. Rev.* **126**, 2030 (1962).

²⁷ F. J. Morin and J. P. Maita, *Phys. Rev.* **129**, 1115 (1963).

²⁸ J. D. Livingston, *Phys. Rev.* **129**, 1943 (1963).

D. Steepness of the Absorption Edge

In Fig. 7 we have plotted the absorption edges of six of our samples. The absorption edges of the remaining samples have been omitted for clarity, since they fall between the curve for 10 at.% tin and that for 10 at.% thallium. Following Richards and Tinkham,⁵ we can show that the absorption curves measure approximately the frequency dependence of $R_N - R_S$, where R_N and R_S are the surface resistances in the normal and the superconducting states, respectively. For comparison with the observed absorption edges, we have plotted the curve showing $R_N - R_S$ derived from the Mattis-Bardeen conductivity values²⁸ in the manner described by Richards and Tinkham.

It is seen from the Figure that the absorption edges for the various lead alloys are much closer to each other than they are to the theoretical curve. This is the same conclusion drawn by Richards and Tinkham from data for other superconductors.²⁹ It should be noted, however, that none of our samples strictly satisfy the conditions for the validity for this application of the theory. These conditions are $\lambda/\xi \ll 1$ and $\omega\tau \ll L/\lambda$, where λ is the penetration depth, ξ is the coherence length, ω is the angular frequency of the radiation, L is the electron mean free path, and τ is the mean-electron scattering time. (See Table II. The manner in which some of the entries were determined is described in the Appendix.) However, the samples which come closest to doing so have absorption curves which are among the most deviant from the theoretical curve. It is interesting that the observed curves agree with each other as well as they do, in light of the large variation in the important parameters which should characterize the samples, as shown in Table II. We have not made any calculations of the theoretical shape of the absorption edge for our samples. This would require an extensive theoretical analysis, since they are expected to be neither in the extreme anomalous limit nor in the classical limit.

E. Structure on the Absorption Curves

The absorption curves in Figs. 3 and 4 all show a small subsidiary absorption peak at an energy of about

²⁹ P. B. Miller [Phys. Rev. **118**, 928 (1960)] has improved on the Mattis-Bardeen calculation by a more precise mathematical treatment of the long-wavelength Fourier components of the currents, for tin and aluminum. His correction in each case makes the theoretical absorption edge slightly less steep. This worsens the agreement with the experimental results of Richards and Tinkham for tin, and also yields a low-temperature absorption edge for aluminum which is slightly less steep than that observed by M. A. Biondi and M. P. Garfunkel [Phys. Rev. **116**, 853 (1959)]. Miller's calculation has not been carried out for lead. P. L. Richards has observed [Phys. Rev. Letters **7**, 412 (1961)] that the absorption edge in tin becomes more steep as one alloys small amounts of indium with the tin, although his results do not show whether the initial onset of absorption is sharp. Richard's samples were electropolished, and it is possible that our purest specimen (No. 7) would have shown a less steep absorption edge than our other samples if the surface had been electropolished to reduce diffuse electron scattering at and near the surface.

0.8 of the gap width. (This statement does not include sample 6, for which an energy gap could not be assigned, and sample 9, for which this region of the absorption curve was not measured.) Some of the curves also show possible structure at about 0.65 of the energy gap.

Such a subsidiary infrared absorption peak has been observed previously in pure lead and mercury,^{4,5} and it was stated that it might be due to either anisotropy or collective states in the gap. Our results seem to weaken both of these possibilities. On the one hand, Anderson²⁴ has shown that significant anisotropy should be present only in samples in which the electron mean free path is not short compared to the coherence length in the pure superconductor. Table II shows that many of our samples do not satisfy this criterion, so anisotropy seems to be ruled out as a possible cause of the observed structure. On the other hand, Maki and Tsuneto³⁰ have calculated the effect of impurity scattering on exciton-like collective states in the gap, and find that scattering should drastically shift the energy of the collective excitation. Since we observe no appreciable shift of this kind, this would indicate that these collective excited states are not the cause of the observed structure. However, it has been suggested³¹ that collective excitations might still explain the structure, if the energy dependence of the gap parameter Δ were taken into account.

To check that the structure was not an instrumental effect, we measured the far infrared absorption of a "dummy sample" cavity made of brass. At any wavelength the absorption ratio " P_S " (magnet off) was found to be equal to the absorption ratio " P_N " (magnet on). This confirms that the structure which we observe in the superconducting samples is not due to a field-induced change in the wavelength dependence of the bolometer's absorption characteristics.

Rowell *et al.*³² have measured electron tunneling between two superconducting lead films. They have found structure in their tunneling curves which they believe is directly related to the observed far infrared structure.

Townsend and Sutton³³ have also found some structure on tunneling curves for lead. They interpret this as resulting from anisotropy. They find two gap values, $4.30 kT_c$ and $4.67 kT_c$. We find a gap width equal to $4.37 kT_c$ in our measurements on almost pure lead (sample No. 7). If we saw their second gap in our measurements, it would occur at approximately 23.8 cm^{-1} . According to Table II, three of our samples 1, 7, and 8, have values of L/ξ_0 large enough to observe anisotropy according to Anderson's criterion.²⁴ How-

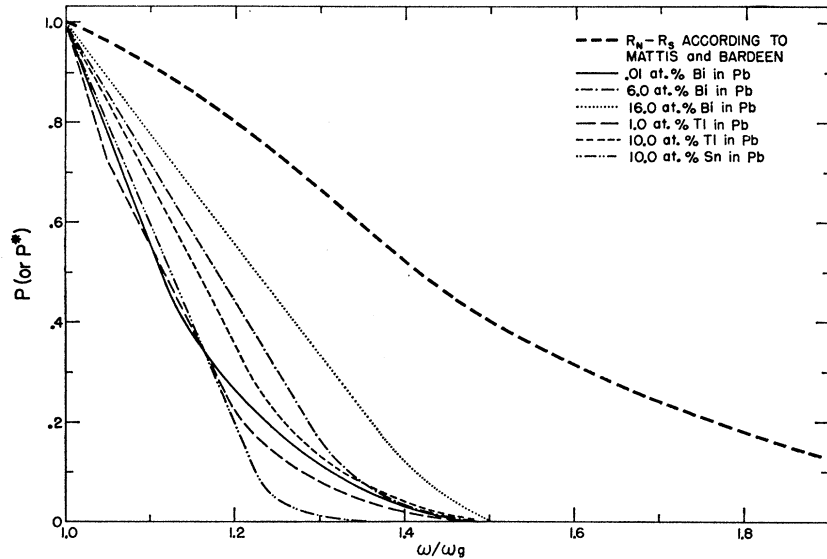
³⁰ K. Maki and T. Tsuneto, Progr. Theoret. Phys. (Kyoto) **28**, 163 (1962).

³¹ L. P. Kadanoff (private communication).

³² J. M. Rowell, P. W. Anderson, and D. E. Thomas, Phys. Rev. Letters **10**, 334 (1963).

³³ P. Townsend and J. Sutton, Phys. Rev. **128**, 591 (1962).

FIG. 7. Absorption edges. The curves indicate values of P except in the case of 16.0 at. % bismuth in lead. For the latter, no normal-state data could be obtained, so the curve indicates values of P^* . P and P^* are defined in the text (Sec. II.E). The absorption edges of the other samples fall between that of 10 at. % tin and that of 10 at. % thallium. The theoretical curve of Mattis and Bardeen was calculated in the extreme anomalous limit, which none of our samples strictly satisfy.



ever, our results do not permit us to confirm the higher gap width found by Townsend and Sutton, which has also been absent in other tunneling measurements.³⁴

IV. SUMMARY

Far infrared absorption measurements for bulk superconducting alloys of lead containing thallium, bismuth, or tin provide for the first time direct experimental evidence of a sharp gap edge in superconducting alloys. We believe this is characteristic of highly homogeneous alloys without trapped magnetic flux.

For each sample, the energy gap width is taken to be the energy at which the absorption curve seems to have a sharp change in slope, and the resulting values are given in Table II. The gap width in almost pure lead (sample 7) is in good agreement with the gap width in "pure" lead which has been found in tunneling measurements.

We have compared the energy gap values for the lead-thallium alloys with observed critical temperatures. For up to 7.7 at. % thallium, alloying decreases the critical temperature and gap width, but the ratio $2\Delta/kT_c$ remains approximately constant at a value of about 4.37. However, at 10.0 at. % thallium, the decrease in gap width is significantly larger than that in the critical temperature, since $2\Delta/kT_c$ is about 4.07. This may indicate that one crosses a band edge on going from 7.7 to 10.0 at. % thallium.

The increase in gap width caused by putting bismuth in lead and the decrease caused by putting thallium in lead call to mind previously observed correlations between solute valence and changes in critical temperature. The absorption curves for both samples composed

of tin in lead are quite sharp, so precipitated tin does not seem to have any drastic effect on the far infrared properties of the superconducting alloy.

The structure on the absorption curve below the gap edge, which has been seen previously in pure lead and mercury, is present in all the alloy samples. This would seem to eliminate anisotropy as a possible cause of the structure. Present theoretical calculations indicate that if the structure is due to exciton-like collective states in the gap, alloying would cause it to shift drastically in energy, contrary to our results.

The steepness of the absorption edge is roughly the same in all of the samples. It is considerably steeper than a theoretical prediction, which however, has been made only in the extreme anomalous limit, which none of our samples strictly satisfy.

ACKNOWLEDGMENTS

We are grateful to P. Handler for the use of some of the equipment used in the preparation of the bolometers. We have profited from discussions with J. Bardeen, L. P. Kadanoff, and D. Markowitz. Thanks go to D. K. Finnemore and D. E. Mapother for permission to use their critical temperature data prior to publication.

APPENDIX: DERIVATION OF SOME OF THE PARAMETERS IN TABLE II

Values for the residual resistivity ρ , which enter into the calculation of some of the parameters in Table II, were obtained for the lead-thallium system by interpolation from data obtained by Goodman.³⁵ These agree quite well with measurements made by Livingston²⁸

³⁴ I. Giaever, H. R. Hart, Jr., and K. Megerle, Phys. Rev. **126**, 941 (1962).

³⁵ B. B. Goodman, IBM J. Res. Develop. **6**, 63 (1962).

at 20.4°K if Matthiessen's rule³⁶ is used to find from these the expected residual resistance values. Residual resistivities for the lead-bismuth and lead-tin samples were estimated from measurements made by Livingston²⁸ on these alloy systems.

The electron mean free path L has been calculated by using the residual resistivity estimates in Chambers' relation³⁷ for lead,

$$(\rho L)^{-1} = (9.4 \pm 0.7) \times 10^{10} \Omega^{-1} \text{ cm}^{-2}.$$

The coherence length ξ in each alloy sample was calculated from Gorkov's equation as simplified by Goodman,³⁵

$$\xi^{-1} = \xi_0^{-1} + (1.32L)^{-1},$$

³⁶ A. H. Wilson, *The Theory of Metals* (Cambridge University Press, New York, 1953).

³⁷ R. G. Chambers, Proc. Roy. Soc. (London) **A215**, 481 (1952).

using a value of 780 Å for ξ_0 . This is the value given by using Bardeen and Schrieffer's value⁹ for the Fermi velocity v , 5×10^7 cm/sec, and our value of Δ for sample 7, in the BCS equation $\xi_0 = \hbar v / \pi \Delta$.

The electron scattering time τ has been estimated from the relation $\tau = L/v$. In Table II, the angular frequency of the radiation ω is that for a wavelength of 500 μ , which is approximately its value at the gap edge.

The penetration depth is estimated from relations given by Pippard,³⁸ which are in approximate agreement with the BCS theory. We calculate his λ_∞ from his Eq. (15), and use our value for ξ_0 and Lock's value³⁹ for λ . Pippard's Eq. (14) then yields a value for Δ . We can then compute λ from his Eq. (13) or (15), or we can obtain λ from his Fig. 2.

³⁸ A. B. Pippard, Proc. Roy. Soc. (London) **A216**, 547 (1953).

³⁹ J. M. Lock, Proc. Roy. Soc. (London) **A208**, 391 (1951).